Dalton Transactions

ROYAL SOCIETY OF CHEMISTRY

PAPER

View Article Online
View Journal | View Issue

Cite this: *Dalton Trans.*, 2025, **54**, 2851

Catalysis activity and chemoselectivity control with the *trans* ligand in Ru–H pincer complexes†

Mita Halder, Diana Castillo Cardenas, ‡ Angela M. Chartouni and Damien B. Culver *

Received 18th December 2024,
Accepted 3rd January 2025

DOI: 10.1039/d4dt03491k

rsc.li/dalton

(PhPN^{H}P)Ru(H)(Cl)(CO) serves as a precatalyst to a variety of important catalytic transformations but most improvements have been restricted to the replacement of the CO ligand *cis* to the hydride or changing the Ph groups of the pincer for other aryl or alkyl groups. The ligand *trans* to the hydride is often another hydride and studies that utilize other *trans* ligands in catalysis are limited. In this work, we synthesized a series of [(PhPN^{H}P)Ru(H)(CO)(L)][BPh$_4$] complexes bearing isonitrile, PMe$_3$, or a N-heterocyclic ligand *trans* to the Ru–H. We compared the new complexes abilities to catalyze the transfer hydrogenation of ketones. We found that all the *trans* ligands improved the chemoselectivity and stability of the catalysts; and strong π-accepting ligands resulted in poor catalytic activities whereas strong σ-donating ligands accelerated the catalysis.

Introduction

Inorganic pincer complexes catalyze a variety of organic transformations, often exhibiting high activities and selectivities.[1–7] (PhPN^{H}P)Ru(H)(Cl)(CO) (also known as Ru–MACHO)[8] and similar analogues serve as precatalysts or catalysts for hydrogenation, transfer hydrogenation, dehydrogenative coupling of alcohols, aldehyde coupling, and other organic transformations.[9–15] In all of these reports, the active catalysts are neutral and the ligand *trans* to the active hydride is another hydride (Fig. 1). Some reports have described (RPN^{H}P)Ru(X)$_2$(L) complexes bearing phosphines, N-heterocyclic carbenes, and other ligands *cis* to the Ru–H instead of CO, or with other R groups on the pincer ligand showing that the ligand choice has a strong effect on the complex's reactivity.[16–20] However, there has been limited work into the formation of active catalysts with ancillary ligands *trans* to the hydride. A method to further examine the effects of ligands *trans* to the hydride is formation of [(RPN^{H}P)Ru(H)(L)$_2$]$^+$ ions which allows for straight forward installation of dative ligands with tunable electronic and steric environments.

Reported examples of monomeric [(RPN^{H}P)Ru(X)(L)$_2$]$^+$ ions (X = H or halide) are limited. Rozenel and Arnold showed that cationic [(^{i}PrPN^{H}P)Ru(Cl)(L)]$^+_2$ dimers can be broken into monomers in the presence of CO.[21] Prakash and coworkers identified [(RPN^{H}P)Ru(X)(CO)$_2$]$^+$ complexes (Fig. 1) as inactive species but can reenter the catalytic cycle in the hydrogenation of CO$_2$ to methanol when starting with (RPN^{H}P)Ru(X)(CO) precursors.[22] Ogata disclosed a patent that utilizes [(RPN^{H}P)Ru(X)(CO)$_2$]$^+$ complexes as catalyst precursors for hydrogenation and *N*-alkylation reactions.[23] Gauvin and coworkers reported the synthesis of [(^{i}PrPN^{H}P)Ru(X)(CNR)$_2$]$^+$ (CNR = isonitrile) complexes (Fig. 1) but did not report any catalysis.[24] Schaub and coworkers showed that [(PhPN^{H}P)Ru(H)(CO)(PR$_3$)][OR(HOR)$_n$] ions (R = Me or Ph) serve as precursors to neutral (PhPNP)Ru(H)(CO)(PR$_3$) complexes that catalyze alcohol dehydrogenation and ester hydrogenation, and are more stable than Ru-MACHO.[25] They attributed the improved stability to stabilization of the active (PhPNP)Ru(H)(CO) by labile phosphines. To

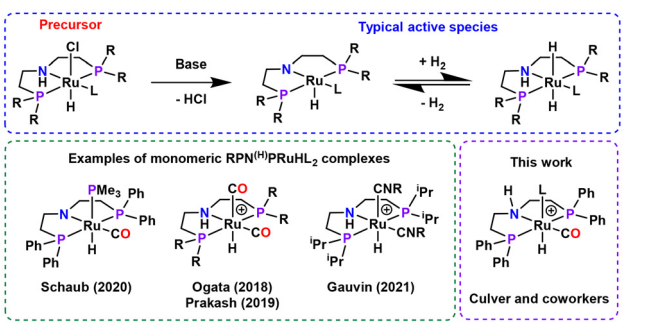

Fig. 1 Top: general scheme for the activation of (RPN^{H}P)Ru(H)(Cl)(L) complexes (R = alkyl or aryl) with a base in the presence of hydrogen source. Bottom left: examples of monomeric (RPN^{H}P)Ru(H)(L)$_2$ complexes. Bottom right: general depiction of the [(PhPN^{H}P)Ru(H)(L)(CO)][BPh$_4$] complexes synthesized in this study.

Division of Chemical and Biological Sciences, Ames National Laboratory, Ames, IA 50011, USA. E-mail: culver@ameslab.gov

†Electronic supplementary information (ESI) available: Other experimental procedures, catalysis and characterization data. CCDC 2392950–2392953. For ESI and crystallographic data in CIF or other electronic format see DOI: https://doi.org/10.1039/d4dt03491k

‡Present address: University of California, Los Angeles, Los Angeles, CA, 90095.

the best of our knowledge, a systematic evaluation of the *trans* ligand influence on the Ru–H in Ru–MACHO derivatives for catalysis has not been previously performed. In this work, we synthesized a series of $[(PhPN^{H}P)Ru(H)(L)(CO)]^{+}$ complexes bearing phosphine, isonitrile and N-heterocyclic ligands and compared their carbonyl transfer hydrogenation activities with neutral Ru–MACHO to determine the effects of dative ligands *trans* to the hydride.

Experimental

General considerations

All procedures were executed under an inert atmosphere of nitrogen or argon utilizing standard Schlenk line or glovebox techniques. THF-d_8 and Benzene-d_6 were purchased from Cambridge Isotope laboratories. Benzene-d_6 was dried over sodium/benzophenone, degassed by three successive freeze–pump–thaw cycles, distilled under vacuum, and stored over 4 Å molecular sieves inside an inert atmosphere glovebox prior to use. THF-d_8 was dried over 4 Å molecular sieves and stored inside an inert atmosphere glovebox prior to use. Anhydrous and degassed solvents were purchased from Sigma Aldrich and stored over 3 or 4 Å molecular sieves prior to use. 1,3,5-Trimethoxybenzene, benzophenone, 4-bromoacetophenone, and 4-methoxyacetophenone were purified by sublimation under vacuum and stored in a glovebox prior to use. Acetophenone was dried over CaH_2 followed by distillation under vacuum. $(PhPN^{H}P)Ru(H)(Cl)(CO)$ (**1**) was purchased from Strem chemicals or Sigma Aldrich and purified prior to use as described in the ESI.† All other commercially available reagents were used as received without further purification.

NMR analyses were performed on a Bruker Avance III 600 MHz spectrometer, or a Varian MR-400 MHz spectrometer housed by the Iowa State University Chemical Instrumentation Facility (CIF). All NMR spectra were obtained at 25 °C unless otherwise specified. All ^{1}H NMR spectra were referenced to the solvent residual signal(s). $^{13}C\{^{1}H\}$ NMR spectra were referenced to a solvent signal. All carbon NMR assignments are singlets unless noted otherwise. The ^{31}P NMR spectra were externally referenced to 85% H_3PO_4 (0.0 ppm). Fourier transform infrared (FTIR) spectra were measured on a Bruker ALPHA II spectrometer contained within an argon filled glovebox. Samples for transmission IR were diluted with KBr and pressed into a transparent pellet using a hand press to make a pellet. Elemental analyses were performed on a Thermo FlashSmart 2000 CHNS/O Combustion Elemental Analyzer housed by the Iowa State University CIF. Single crystal diffraction data was collected using a Bruker D8 VENTURE diffractometer using MoKα (λ = 0.71073) in the ISU CIF.

Synthesis of complexes 2a–d, 3, and 4

$[(PhPN^{H}P)Ru(H)(\mathbf{CNCy})(CO)][BPh_4]$ (**2a**): In a 25 mL Schlenk tube, **1** (100.0 mg, 0.165 mmol) in 10 mL tetrahydrofuran (THF) was stirred at 65 °C until complete dissolution. Then CyNC (22.5 μL, 0.181 mmol) was added and the reaction was stirred at 65 °C for 10 h. $NaBPh_4$ (56.4 mg, 0.165 mmol) was added and after 1 h of additional stirring at 65 °C, the mixture was cooled to room temperature, filtered through Celite and concentrated to 5 mL under reduced pressure. A layer of pentane (5 mL) was added, and the solution was kept overnight at room temperature resulting in 89.0 mg of a colorless needle shaped microcrystalline product. The product was isolated by filtration, washed with pentane and finally dried under vacuum. The mother liquor was reduced to 2 mL and further recrystallized using pentane (2 mL) furnishing another 36.0 mg of the microcrystalline product. Total yield of **2a** was 125.0 mg (76%). **^{1}H NMR (THF-d_8, 25 °C, 600 MHz):** δ 7.88–7.85 (m, 4H, Ph**H**), 7.67–7.64 (m, 4H, Ph**H**), 7.51–7.44 (m, 12H, Ph**H**), 7.32 (bs, 8H, Ph**H** in BPh_4), 6.86 (t, $^{3}J_{HH}$ = 7.4 Hz, 8H, Ph**H** in BPh_4), 6.71 (t, $^{3}J_{HH}$ = 7.2 Hz, 4H, Ph**H** in BPh_4), 3.75–3.71 (m, 1H, $CH_2N\mathbf{H}CH_2$), 3.35 (m, 1H, *ipso* **H** in Cyclohexane), 2.94–2.85 (m, 2H, $NC\mathbf{H}_2CH_2P$), 2.81–2.77 (m, 2H, $NCH_2C\mathbf{H}_2P$), 2.19 (td, $^{2}J_{PH}$ = 14.5, $^{3}J_{HH}$ = 4.6 Hz, 2H, $NCH_2C\mathbf{H}_2P$), 2.14–2.08 (m, 2H, $NC\mathbf{H}_2CH_2P$), 1.38–1.28 (m, 5H, Cyclohexyl $C\mathbf{H}_2$), 1.14–0.97 (m, 5H, Cyclohexyl $C\mathbf{H}_2$), −7.65 (t, $^{2}J_{PH}$ = 17.01 Hz, 1H, Ru–**H**) ppm. **$^{31}P\{^{1}H\}$ NMR (THF-d_8, 25 °C, 242.9 MHz):** 57.5 (s, Ru–P) ppm. **$^{13}C\{^{1}H\}$ NMR (THF-d_8, 25 °C, 150.9 MHz):** 203.8 (Ru–**C**O, identified by HMBC), 165.4 (q, $^{1}J_{CB}$ = 49.3 Hz, C_i of BPh_4), 147.6 (Ru–**C**NR, identified by HMBC), 137.4 (bs, *ortho* C of BPh_4), 137.3 (t, $^{1}J_{PC}$ = 22.6 Hz, P–Ph, C_i), 135.9 (t, $^{1}J_{PC}$ = 22.6 Hz, PPh, C_i), 134.1 (t, $^{2}J_{PC}$ = 6.8 Hz, PPh), 132.8 (t, $^{2}J_{PC}$ = 6 Hz, PPh), 131.7, 131.4, 130 (t, $^{3}J_{PC}$ = 4.5 Hz, PPh), 129.7 (t, $^{3}J_{PC}$ = 5.3 Hz, PPh), 126.1 (q, $^{3}J_{CB}$ = 3 Hz, *meta* C of BPh_4), 122.2 (bs, *para* C of BPh_4), 55.3 (**C**HNC), 54.8 ($PCH_2\mathbf{C}H_2N$), 33.9 (t, $^{1}J_{PC}$ = 13.6 Hz, $NCH_2\mathbf{C}H_2P$), 33.1, 23.7 ppm. **FTIR (cm^{-1}):** 2172 ($\nu_{C\equiv N}$), 1953 ($\nu_{C=O}$). **Elemental analysis** calculated for $C_{60}H_{61}BN_2OP_2Ru$: C = 72.07%, H = 6.15%, N = 2.80%, found: C = 72.50%, H = 6.69%, N = 2.81%.

$[(PhPN^{H}P)Ru(H)(\mathbf{CN^{t}Bu})(CO)][BPh_4]$ (**2b**) was synthesized following the similar manner to **2a**. Reaction of **1** (100 mg, 0.165 mmol) in THF (10 mL) with ^{t}BuNC (20.5 μL, 0.181 mmol) and $NaBPh_4$ (56.4 mg, 0.165 mmol), followed by recrystallization yielded the white needle shaped microcrystal as the final product. Yield: 119.0 mg, (74%). **^{1}H NMR (THF-d_8, 25 °C, 600 MHz):** δ 7.88–7.84 (m, 4H, Ph**H**), 7.69–7.66 (m, 4H, Ph**H**), 7.53–7.44 (m, 12H, Ph**H**), 7.34–7.31 (m, 8H, Ph**H** in BPh_4), 6.86 (t, $^{3}J_{HH}$ = 6 Hz, 8H, Ph**H** in BPh_4), 6.71 (t, $^{3}J_{HH}$ = 6 Hz, 4H, Ph**H** in BPh_4), 3.73 (bs, 1H, $N\mathbf{H}CH_2CH_2P$), 2.93–2.83 (m, 2H, $NHC\mathbf{H}_2CH_2P$), 2.80–2.76 (m, 2H, $PC\mathbf{H}_2CH_2N$), 2.19 (td, $^{2}J_{PH}$ = 15 Hz, $^{3}J_{HH}$ = 6 Hz, 2H, $PC\mathbf{H}_2CH_2N$), 2.15–2.09 (m, 2H, $NC\mathbf{H}_2CH_2P$), 0.91 (s, 9H, $C(C\mathbf{H}_3)_3$), −7.63 (t, $^{2}J_{PH}$ = 15 Hz, 1H, Ru–**H**) ppm. **$^{31}P\{^{1}H\}$ NMR (THF-d_8, 25 °C, 242.9 MHz):** 57.6 (s, Ru–P) ppm. **$^{13}C\{^{1}H\}$ NMR (THF-d_8, 25 °C, 150.9 MHz**): 203.5 (Ru–**C**O, identified by HMBC), 165.4 (q, $^{1}J_{CB}$ = 49.3 Hz, C_i of BPh_4), 145.8 (Ru–**C**NR, identified by HMBC), 137.5 (t, $^{1}J_{PC}$ = 22.8 Hz, P–Ph, C_i) 137.4 (bs, *ortho* C of BPh_4,), 135.8 (t, $^{1}J_{PC}$ = 24.5 Hz, PPh, C_i), 134.1 (t, $^{2}J_{PC}$ = 6.8 Hz, PPh), 132.8 (t, $^{2}J_{PC}$ = 6 Hz, PPh), 131.7, 131.5, 130.1 (t, $^{3}J_{PC}$ = 5.3 Hz, PPh), 129.7 (t, $^{3}J_{PC}$ = 5.3 Hz, PPh), 126.1 (q, $^{3}J_{CB}$ = 2.5 Hz, *meta* C of BPh_4,), 122.2 (bs, *para* C of BPh_4,), 58.4 ($Me_3\mathbf{C}NC$), 54.8 (t, $^{2}J_{PC}$ = 4.5 Hz, $PCH_2\mathbf{C}H_2NH$), 33.9 (t, $^{1}J_{PC}$ = 13.6 Hz, $NCH_2\mathbf{C}H_2P$),

30.2 ppm (C(CH$_3$)$_3$). **FTIR (cm^{-1}):** 2163 ($\nu_{C\equiv N}$), 1947 ($\nu_{C=O}$). **Elemental analysis calculated for $C_{58}H_{59}BN_2OP_2Ru$:** C = 71.53%, H = 6.11%, N = 2.88%, Found: C = 71.57%, H = 6.34%, N = 2.79%.

[(PhPN^{H}P)Ru(H)(**CN^{n}Bu**)(CO)][BPh$_4$] (**2c**) was synthesized following the similar manner to **2a**. Reaction of **1** (100 mg, 0.165 mmol) in THF (10 mL) with ^{n}BuNC (19.0 μL, 0.181 mmol) and NaBPh$_4$ (56.4 mg, 0.165 mmol), followed by recrystallization yielded the white microcrystals as the final product. Yield: 114.0 mg, (71%). **^{1}H NMR (THF-d_8, 25 °C, 600 MHz):** δ 7.87–7.83 (m, 4H, PhH), 7.66–7.63 (m, 4H, PhH), 7.50–7.43 (m, 12H, PhH), 7.32–7.29 (m, 8H, PhH in BPh$_4$), 6.85 (t, $^3J_{HH}$ = 7.4 Hz, 8H, PhH in BPh$_4$), 6.71 (t, $^3J_{HH}$ = 7.1 Hz, 4H, PhH in BPh$_4$), 3.81 (bs, 1H, NHCH$_2$CH$_2$P), 3.06 (t, $^3J_{HH}$ = 6.7 Hz, 2H, CH$_2$NC), 2.96–2.87 (m, 2H, NCH$_2$CH$_2$P), 2.83–2.79 (m, 2H, PCH$_2$CH$_2$N), 2.22–2.16 (m, 2H, PCH$_2$CH$_2$N), 2.15–2.10 (m, 2H, NHCH$_2$CH$_2$P), 1.10–1.06 (m, 2H, CH$_2$ of ^{n}BuNC), 0.98–0.92 (m, 2H, CH$_2$ of ^{n}BuNC), 0.72 (t, $^3J_{HH}$ = 7.3 Hz, 3H, CH$_3$CH$_2$), −7.71 (t, $^2J_{PH}$ = 17.1 Hz, 1H, Ru–H) ppm.

^{31}P{^{1}H} NMR (THF-d_8, 25 °C, 242.9 MHz). 57.7 (s, Ru–P) ppm. **^{13}C{^{1}H} NMR (THF-d_8, 25 °C, 150.9 MHz):** 202.6 (Ru–CO, identified by HMBC), 164.3 (q, $^1J_{CB}$ = 49.4 Hz, C$_i$ of BPh$_4$), 147.2 (Ru–CNR, identified by HMBC), 136.2 (bs, *ortho* C of BPh$_4$), 136.0 (t, $^1J_{PC}$ = 22.9 Hz, P–Ph, C$_i$), 134.8 (t, $^1J_{PC}$ = 24.3 Hz, PPh, C$_i$), 132.8 (t, $^2J_{PC}$ = 6.9 Hz, PPh), 131.6 (t, $^2J_{PC}$ = 6.1 Hz, PPh), 130.6, 130.3, 128.8 (t, $^3J_{PC}$ = 4.9 Hz, PPh), 128.5 (t, $^3J_{PC}$ = 5.2 Hz, PPh), 124.9 (q, $^3J_{CB}$ = 2.9 Hz, *meta* C of BPh$_4$), 120.9 (bs, *para* C of BPh$_4$), 53.8 (t, $^2J_{PC}$ = 4.6 Hz, PCH$_2$CH$_2$N), 43.3 (CH$_2$NC), 32.8 (t, $^1J_{PC}$ = 13.3 Hz, NCH$_2$CH$_2$P), 30.5 (CH$_2$CH$_2$NC of ^{n}BuNC), 19.2 (CH$_3$CH$_2$CH$_2$ of ^{n}BuNC), 12.6 (CH$_3$CH$_2$CH$_2$) ppm. **FTIR (cm^{-1}):** 2185 ($\nu_{C\equiv N}$), 1961 ($\nu_{C=O}$). **Elemental analysis calculated for $C_{58}H_{59}BN_2OP_2Ru$:** C = 71.53%, H = 6.11%, N = 2.88%, Found: C = 72.93%, H = 6.07%, N = 2.97%.

[(PhPN^{H}P)Ru(H)(**CNBn**)(CO)][BPh$_4$] (**2d**) was synthesized following the similar manner to **2a**. **1** (100 mg, 0.165 mmol) in THF (10 mL) was stirred with Benzyl isonitrile (22.0 μL, 0.181 mmol) for 20 h at 65 °C, then additional 1 h stirring with NaBPh$_4$ (56.4 mg, 0.165 mmol), followed by recrystallization yielded the pale-yellow microcrystal as the final product. Yield: 111.0 mg, (67%). **^{1}H NMR (THF-d_8, 25 °C, 600 MHz):** δ 7.87–7.83 (m, 4H, PhH), 7.68–7.64 (m, 4H, PhH), 7.45–7.44 (m, 12H, PhH), 7.33–7.2 (m, 13H, PhH in BPh$_4$ and PhCH$_2$), 6.83 (t, $^3J_{HH}$ = 9 Hz, 8H, PhH in BPh$_4$), 6.70 (q, $^3J_{HH}$ = 6 Hz, 4H, PhH in BPh$_4$), 4.34 (s, CH$_2$Ph), 3.90 (bs, 1H, NHCH$_2$CH$_2$P), 2.96–2.81 (m, 4H, NCH$_2$CH$_2$P), 2.20–2.13 (m, 4H, NCH$_2$CH$_2$P), −7.62 (t, $^2J_{PH}$ = 15 Hz, 1H, Ru–H) ppm. **^{31}P{^{1}H} NMR (THF-d_8, 25 °C, 242.9 MHz):** 58.9 (s, Ru–P) ppm. **^{13}C{^{1}H} NMR (THF-d_8, 25 °C, 150.9 MHz):** 203.5 (Ru–CO, identified by HMBC), 165.4 (q, $^1J_{CB}$ = 49.3 Hz, C$_i$ of BPh$_4$), 149.9 (Ru–CNR, identified by HMBC), 137.4 (d, $^2J_{CB}$ = 3 Hz, *ortho* C of BPh$_4$), 136.9 (t, $^1J_{PC}$ = 23.4 Hz, PPh, C$_i$), 135.9 (t, $^1J_{PC}$ = 24.9 Hz, PPh, C$_i$), 133.9 (t, $^2J_{PC}$ = 6.8 Hz, PPh), 133.4 (PhCH$_2$NC), 132.8 (t, $^2J_{PC}$ = 6 Hz, PPh), 131.7, 131.6, 130.1 (t, $^3J_{PC}$ = 5.3 Hz, PPh), 129.9 (PhCH$_2$NC), 129.7 (t, $^3J_{PC}$ = 5.3 Hz, PPh), 129.3 (PhCH$_2$NC), 127.6 (PhCH$_2$NC), 126.0 (q, $^3J_{CB}$ = 2.5 Hz, *meta* C of BPh$_4$), 122.2 (bs, *para* C of BPh$_4$), 54.9 (t, $^2J_{PC}$ = 4.5 Hz, PCH$_2$CH$_2$NH), 48.2 (PhCH$_2$NC), 34.0 (t, $^1J_{PC}$ = 12.8 Hz, NCH$_2$CH$_2$P) ppm. **FTIR (cm^{-1}):** 2178 ($\nu_{C\equiv N}$), 1961 ($\nu_{C=O}$). **Elemental analysis calculated for $C_{61}H_{57}BN_2OP_2Ru$:** C = 72.69%, H = 5.70%, N = 2.78%, Found: C = 72.90%, H = 5.75%, N = 4.08%. The found N percentage for **4** did not improve after multiple attempts to obtain satisfactory elemental analysis. Although these results are outside the range viewed as establishing analytical purity, they are provided to illustrate the best values obtained to date.

[(PhPN^{H}P)Ru(H)(**PMe$_3$**)(CO)][BPh$_4$] (**3**) was synthesized following the similar manner to **2a**. **1** (200 mg, 0.33 mmol) in THF (20 mL) was stirred with PMe$_3$ (38.0 μL, 0.363 mmol) for 2 h at 65 °C, then additional 1 h stirring with NaBPh$_4$ (56.4 mg, 0.165 mmol) at the same temperature, followed by recrystallization yielded pale-yellow microcrystals as the final product. Yield: 258 mg, (81%). **^{1}H NMR (THF-d_8, 25 °C, 600 MHz):** δ 8.01–7.98 (m, 4H, PhH), 7.67–7.64 (m, 4H, PhH), 7.49–7.41 (m, 12H, PhH), 7.31–7.29 (m, 8H, PhH in BPh$_4$), 6.85 (t, $^3J_{HH}$ = 7.44 Hz, 8H, PhH in BPh$_4$), 6.71 (t, $^3J_{HH}$ = 7.14 Hz, 4H, PhH in BPh$_4$), 3.70 (bs, 1H, NHCH$_2$CH$_2$P), 3.10–3.01 (m, 2H, NCH$_2$CH$_2$P), 2.91–2.88 (m, 2H, PCH$_2$CH$_2$N), 2.19 (td, $^2J_{PH}$ = 14.7 Hz, $^3J_{HH}$ = 5.04 Hz, 2H, PCH$_2$CH$_2$N), 2.01–1.98 (m, 2H, NCH$_2$CH$_2$P), 0.73 (d, $^2J_{PH}$ = 7.2 Hz, 9H, PMe$_3$), −7.38 (dt, $^2J_{PH}$ = 85.6 Hz (*trans* PMe$_3$), $^2J_{PH}$ = 18.8 Hz (*cis* PPh$_2$), 1H, Ru–H) ppm. **^{31}P{^{1}H} NMR (THF-d_8, 25 °C, 242.9 MHz):** 56.5 (d, $^2J_{PP}$ = 16.8 Hz, Ru–PPh$_2$), −26.8 (t, $^2J_{PP}$ = 17.8 Hz, Ru–PMe$_3$) ppm. **^{13}C{^{1}H} NMR (THF-d_8, 25 °C, 150.9 MHz):** 205.8 (Ru–CO, identified by HMBC), 165.4 (q, $^1J_{CB}$ = 49.3 Hz, C$_i$ of BPh$_4$), 138.2 (t, $^1J_{PC}$ = 22.7 Hz, P–Ph, C$_i$), 137.6 (P–Ph, C$_i$), 137.4 (s, *ortho* C of BPh$_4$), 134.2 (t, $^2J_{PC}$ = 6.6 Hz, PPh), 132.2 (t, $^2J_{PC}$ = 6 Hz, PPh), 131.5 (d, $^1J_{PC}$ = 14.2 Hz, PPh, C$_i$), 130.5 (t, $^3J_{PC}$ = 4.6 Hz, PPh), 129.6 (t, $^3J_{PC}$ = 5.2 Hz, PPh), 125.9 (q, $^3J_{CB}$ = 2.8 Hz, *meta* C of BPh$_4$), 122.2 (bs, *para* C of BPh$_4$), 54.1 (PCH$_2$CH$_2$N), 32.9 (t, $^1J_{PC}$ = 13.0 Hz, NCH$_2$CH$_2$P), 17.8 (d, $^1J_{PC}$ = 23.5 Hz, PMe$_3$) ppm. **FTIR (cm^{-1}):** 1941 ($\nu_{C=O}$). **Elemental analysis calculated for $C_{56}H_{59}BNOP_3Ru$:** C = 69.56%, H = 6.15%, N = 1.45%, Found: C = 68.61%, H = 6.38%, N = 2.00%.

[(PhPN^{H}P)Ru(H)(NHC)(CO)][BPh$_4$] (4). 1,3-Dimethylimidazolium-2-carboxylate reacts slowly with **1**, therefore, **4** was synthesized by a different method. **1** (100 mg, 0.165 mmol) in THF (10 mL) was stirred with NaBPh$_4$ (56.4 mg, 0.165 mmol) at 65 °C for 1 h. Then 1,3-dimethylimidazolium-2-carboxylate (25.6 mg, 0.181 mmol) was added, and the reaction mixture was stirred for 24 h at 75 °C. After completion of the reaction, the pale-yellow microcrystalline pure product was collected by recrystallization from 1 : 1 mixture of THF and pentane. Yield: 121 mg, (74%). **^{1}H NMR (THF-d_8, 25 °C, 600 MHz):** δ 7.87–7.84 (m, 4H, PhH), 7.47–7.46 (m, 5H, PhH), 7.35–7.29 (m, 8H, PhH in BPh$_4$, 3H, PhH), 7.19 (t, $^3J_{HH}$ = 7.59 Hz, 4H, PhH), 6.99–6.96 (m, 4H, PhH), 6.85 (t, $^3J_{HH}$ = 7.35 Hz, 8H, *meta* PhH in BPh$_4$), 6.71 (t, $^3J_{HH}$ = 7.29 Hz, 4H, *para* PhH in BPh$_4$), 6.68 (broad shoulder, 2H, NCHCHN), 4.00 (bs, 1H, NHCH$_2$CH$_2$P), 3.32–3.25 (m, 2H, NCH$_2$CH$_2$P), 3.09 (bs, 2H, PCH$_2$CH$_2$N), 2.91 (s, 6H, NCH$_3$), 2.46–2.39 (m, 2H, PCH$_2$CH$_2$N, 2H, NCH$_2$CH$_2$P), −8.98 (t, $^2J_{PH}$ = 18.4 Hz, 1H, Ru–H) ppm. **^{1}H NMR (THF-d_8, 50 °C, 600 MHz):** δ

7.86–7.83 (m, 4H, Ph**H**), 7.46–7.44 (m, 4H, Ph**H**), 7.34–7.29 (m, 8H, Ph**H** in BPh_4, 3H, Ph**H**), 7.19 (t, $^3J_{HH}$ = 7.6 Hz, 4H, Ph**H**), 6.99–6.97 (m, 4H, Ph**H**), 6.85 (t, $^3J_{HH}$ = 7.35 Hz, 8H, *meta* Ph**H** in BPh_4), 6.71 (t, $^3J_{HH}$ = 7.29 Hz, 4H, *para* Ph**H** in BPh_4), 6.65 (s, 2H, NC**H**C**H**N), 3.93 (bs, 1H, N**H**CH_2CH_2P), 3.31–3.23 (m, 2H, NC**H**$_2CH_2P$), 3.13–3.12 (m, 2H, PC**H**$_2CH_2N$), 2.91 (s, 6H, NC**H**$_3$), 2.45–2.35 (m, 2H, PC**H**$_2$C**H**$_2$N, 2H, NC**H**$_2CH_2P$), −9.02 (t, $^2J_{PH}$ = 18.4 Hz, 1H, Ru–**H**) ppm. **$^{31}P\{^1H\}$ NMR (THF-d_8, 25 °C, 242.9 MHz):** 59.5 ppm. **$^{13}C\{^1H\}$ NMR (THF-d_8, 25 °C, 150.9 MHz):** 207.1 (Ru–**C**O, identified by HMBC), 184.6 (MeN**C**NMe identified by HMBC), 165.3 (q, $^1J_{CB}$ = 49.2 Hz, C_i of BPh_4), 137.3 (bs, *ortho* C of BPh_4), 136.9 (t, $^1J_{PC}$ = 20.2 Hz, PPh, C_i), 136.8 (t, $^1J_{PC}$ = 24.5 Hz, PPh, C_i), 134.4 (t, $^2J_{PC}$ = 6.6 Hz, PPh), 132.7 (t, $^2J_{PC}$ = 5.8 Hz, PPh), 131.5, 130.9, 129.5–129.4 (P**Ph**), 126.05–125.9 (m, *meta* C of BPh_4), 124.5 (N**C**H**C**HN), 122.2 (*para* C of BPh_4), 55.8 (t, $^2J_{PC}$ = 4.2 Hz, PCH$_2$**C**H$_2$N), 39.4 (N**C**H$_3$), 35.9 (t, $^1J_{PC}$ = 12.5 Hz, P**C**H$_2$CH$_2$N) ppm. **FTIR (cm^{-1}):** 1931 ($\nu_{C=O}$). **Elemental analysis calculated for $C_{58}H_{58}BN_3OP_2Ru$:** C = 70.58%, H = 5.92%, N = 4.26%, Found: C = 70.03%, H = 6.2%, N = 5.49%.

General procedure for the transfer hydrogenation catalysis

In an NMR tube, ketone (0.15 mmol), catalyst (stock solution in THF), KO^{t}Bu (stock solution in THF), a benzene-d_6 capillary and ^{i}PrOH (0.4 mL), were added under nitrogen atmosphere and then heated at 80 °C for the specified period. Afterwards, the reaction mixture was cooled to room temperature. 1,3,5-Trimethoxybenzene was added to the reaction mixture as an internal standard and the reactions were analyzed by ^{1}H NMR spectroscopy. The reaction conditions for Tables 1 and 2 in the main text were chosen based on conditions optimized with **2a** for benzophenone reduction as shown in Table S1.† Representative time course NMR measurements for benzophenone transfer hydrogenation are provided in Fig. S2–S6† for **1**, **2a**, **2d**, **3** and **4**.

Catalysis in the presence of excess ligand

Five equiv. of ligand. A mixture of benzophenone (0.15 mmol), **2a** or **3** (0.15 μmol, 0.1 mol%), KO^{t}Bu (0.94 μmol, 0.625 mol%), ligand (0.75 μmol, CNCy for **2a** or PMe_3 for **3**), ^{i}PrOH (0.4 mL), and THF-d_8 (0.15 mL) in an NMR tube was heated at 80 °C for the indicated time in Table 3 then analyzed by NMR spectroscopy.

One equiv. of PMe_3. A mixture of **3** (3 μmol, 2 mol%), KO^{t}Bu (7.5 μmol, 5 mol%), ^{i}PrOH (0.4 mL), PMe_3 (3 μmol) and THF-d_8 (0.15 mL) in an NMR tube was heated for 10 min at 80 °C. Then benzophenone (0.15 mmol) was added, and the tube was heated at 80 °C for an additional 30 min then analyzed by NMR spectroscopy.

Attempt to generate catalyst 3 *in situ*. A mixture of 1 (0.75 μmol, 1 equiv.), PMe_3 (0.75 μmol, 1 equiv.), $NaBPh_4$ (0.75 μmol, 1 equiv.) in THF-d_8 were combined in an NMR tube and occasionally sonicated for 30 minutes at room temperature. Then benzophenone (0.25 mmol), KO^{t}Bu (1.6 μmol) and ^{i}PrOH (0.4 mL) were added to that tube. After sonication for 5 minutes at room temperature the tube was heated at 80 °C for the indicated time in Table 3 and progress of the reaction was monitored by NMR spectroscopy.

Complex speciation under catalysis conditions

A mixture of **1**, **2b** or **3** (3 μmol, 2 mol%), KO^{t}Bu (7.5 μmol, 5 mol%), ^{i}PrOH (0.4 mL) and THF-d_8 in an NMR tube was analyzed by NMR spectroscopy after sonication at room temperature for 5 min. After 30 min heating at 80 °C the mixture was again analyzed by NMR spectroscopy. Then benzophenone (0.15 mmol) was added, and the tube was heated at 80 °C for an additional 30 min. After cooling down the reaction mixture was analyzed by NMR spectroscopy (Fig. S13–S21†). The reactions with **1** are complicated and contain many species that change at each step. The major species observed in the reactions with **2b** and **3** are assigned to **2b′** and **3′**, respectively. NMR chemical shifts of observed species are provided below.

Relevant NMR signals for **2b′**: ^{1}H NMR (THF-d_8, 25 °C, 400 MHz): −7.54 (bt, $^2J_{PH}$ = 18 Hz, 1H, Ru–**H**) ppm. $^{31}P\{^1H\}$ NMR (THF-d_8, 25 °C, 161.9 MHz): 57.7 ppm.

Relevant NMR signals for **3′**:**^{1}H NMR (THF-d_8, 25 °C, 400 MHz):** −7.41 (dt, $^2J_{PH}$ = 85.7 Hz, $^2J_{PH}$ = 19.0 Hz (*cis* PPh_2), ^{1}H, Ru–**H**) ppm. **$^{31}P\{^1H\}$ NMR (THF-d_8, 25 °C, 161.9 MHz):** 56.0 (d, $^2J_{PP}$ = 18 Hz for Ru–**P**Ph_2), −27.7 ppm (t, $^2J_{PP}$ = 18 Hz, Ru–**P**Me_3) ppm.

Ligand exchange studies

A mixture of **2a** or **4** (10 μmol, 1 equiv.), ^{i}PrOH (300 μmol, 30 equiv.), and PMe_3 (11 μmol, 1.1 equiv.) in THF-d_8 (0.15 mL) combined in an NMR tube and heated at 80 °C for 30 minutes. After analyzing by NMR spectroscopy, KO^{t}Bu (10 μmol, 1 equiv.) was added to the reaction mixture and further heated at 80 °C for 30 minutes. After cooling the reaction mixtures were analyzed by NMR spectroscopy (Fig. S83–S88†).

Relevant NMR signals for **2a** + **PMe_3**: **^{1}H NMR (THF-d_8, 25 °C, 400 MHz):** −7.58 (t, $^2J_{PH}$ = 18.1 Hz, 1H, Ru–**H** of **2a′**), −7.58 (dt, $^2J_{PH}$ = 90. Hz, $^2J_{PH}$ = 18.4 Hz (*cis* PPh_2), ^{1}H, Ru–**H**), −7.60 (t, $^2J_{PH}$ = 19.7 Hz, 1H, Ru–**H** of **2a′**) ppm. **$^{31}P\{^1H\}$ NMR (THF-d_8, 25 °C, 161.9 MHz):** 62.2 (s, for Ru–**P**Ph_2 of unknown species), 58.7 (s, **2a′**), 58.5 (d, $^2J_{PP}$ = 18 Hz, Ru–**P**Me_3 of **3′**), −27.9 (t, $^2J_{PP}$ = 18 Hz, Ru–**P**Me_3 of **3′**) ppm.

Relevant NMR signals for **4** + **PMe_3**:**^{1}H NMR (THF-d_8, 25 °C, 400 MHz):** −7.6 (dt, $^2J_{PH}$ = 90.5 Hz, $^2J_{PH}$ = 18.9 Hz, 1H, Ru–H of **3′**), −9.0 (t, $^2J_{PH}$ = 18.4 Hz, 1H, Ru–H of **4′**), −13.2 (t, $^2J_{PH}$ = 17.9 Hz, Ru–H of unknown species) ppm. **$^{31}P\{^1H\}$ NMR (THF-d_8, 25 °C, 161.9 MHz):** 61.8 (d, $^2J_{PP}$ = 8 Hz, Ru–**P**Ph_2 of unknown species), 60.9 (d, $^2J_{PP}$ = 34.2 Hz, Ru–**P**Ph_2 of unknown species), 58.9 (bs, Ru–**P**Ph_2 of **3′** + **4′**), −20.5 (s, Ru–**P**Me_3 of unknown species), −28.0 ppm (bs, Ru–**P**Me_3 of **3′** + unknown species) ppm.

Results and discussion

Syntheses and characterization

As shown in Scheme 1, the [(PhPN^{H}P)Ru(H)(L)(CO)][BPh_4] complexes, where L is CyNC (**2a**), ^{t}BuNC (**2b**), ^{n}BuNC (**2c**), BnNC (**2d**), PMe_3 (**3**), and N-heterocyclic carbene

Table 1 Summary of the comparative catalytic transfer hydrogenation of benzophenone reactions[a]

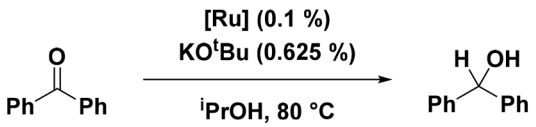

Entry	Catalyst	Time (h)	Consumption[b] (%)	Yield[b] (%)	Selectivity[c] (%)
1	**1**	5.5	98.9 (±0.6)	96.6 (±1.5)	98 (±2)
2	**2a**	5.5	99.2 (±0.3)	97 (±1)	98 (±1)
3	**2b**	4	99.4 (±0.2)	98.2 (±0.4)	98.8 (±0.6)
4	**2c**	4	98.7 (±0.8)	95.4 (±0.2)	97 (±1)
5	**2d**	24	98.8 (±0.6)	88.9 (±0.9)	90 (±1)
6	**3**	1.5	99.6 (±0.2)	98.9 (±0.5)	99.3 (±0.7)
7	**4**	1.5	99.4 (±0.4)	98 (±1)	99 (±1)

[a] Reaction conditions: benzophenone (0.15 mmol), ^{i}PrOH (0.4 mL), catalyst (0.1 mol%), and KO^{t}Bu (0.625 mol%) were combined in an NMR tube and heated at 80 °C. [b] Consumptions of benzophenone and yields of diphenylmethanol were determined by ^{1}H NMR spectroscopy in the presence of 1,3,5-trimethoxybenzene as an internal standard and performed in duplicate. The values reported are averages and the errors are provided in the parentheses. [c] (Yield/consumption) × 100. Absolute errors are provided in the parentheses.

Table 3 Summary of the catalytic transfer hydrogenation of benzophenone reactions in the presence of excess ligand or *in situ* catalyst generation attempts[a]

Entry	Catalyst	Additive(s) (equiv.)	Time (h)	Consumption[b] (%)	Yield[b] (%)
1	**1**	PMe_3 (1.4)	6	19.9	18.8
2	**1**	PMe3 (1) + $NaBPh_4$ (1)	1.5	0	0
3	**2a**	CNCy (5)	1.2	0	0
4	**3**	PMe_3 (5)	0.7	0	0
5[c]	**3**	PMe_3 (1)	0.5	38.4	37.1
6[c]	**3**	None	0.5	>99	93

[a] Reaction conditions: benzophenone (0.15 mmol), ^{i}PrOH (0.4 mL), catalyst (0.1 mol%), additive (s), and KO^{t}Bu (0.625 mol%) were combined in an NMR tube and heated at 80 °C. [b] Consumptions of benzophenone and yields of diphenylmethanol were determined by ^{1}H NMR spectroscopy in the presence of 1,3,5-trimethoxybenzene as an internal standard. [c] Reaction conditions: benzophenone (0.15 mmol), ^{i}PrOH (0.4 mL), catalyst (2 mol%), additive, and KO^{t}Bu (5 mol%) were combined in an NMR tube and heated at 80 °C.

$(C(N(Me)CH)_2$, NHC) (**4**), were synthesized *via* ligand substitution of the chloride and anion exchange. For the synthesis of complexes **2a–d**, and **3**, **1** was treated with the appropriate ligand to furnish [(PhPN^{H}P)Ru(H)(L)(CO)]Cl, followed by addition of $NaBPh_4$ to exchange the outer sphere Cl anion with the weakly – coordinating BPh_4 anion. Complex **4** was synthesized utilizing 1,3-dimethylimidazolium-2-carboxylate which releases CO_2 and forms 1,3-dimethylimidazole *in situ*, a similar approach was utilized by Ogata, Kayaki, and coworkers to synthesize (PhPN^{H}P)Ru(Cl)$_2$(NHC).[17] Attempts to displace the Cl anion following a similar method that was utilized for **2a–d** and **3** resulted in incomplete conversion and a mere 30% of [(PhPN^{H}P)Ru(H)(NHC)(CO)]Cl complex formation after 48 h in refluxing THF. Reversing the order of addition leads to formation of a poorly soluble solid that is likely the hydride bridged dimer [(PhPN^{H}P)Ru(H)(CO)]$_2$[BPh_4]$_2$.[21,26] Addition of 1,3-dimethylimidazolium-2-carboxylate to the solid led to full conversion to **4** in refluxing THF overnight. The structures of

Table 2 Summary of the catalytic transfer hydrogenation substrate scope[a]

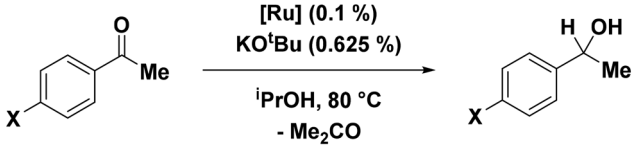

Entry	Catalyst	X	Time (h)	Consumption[b] (%)	Yield[b] (%)	Selectivity[c] (%)
1	**1**	Br	2	98 (±1)	61 (±1)	62 (±2)
2	**2a**		2	97 (±1)	70 (±2)	72 (±3)
3	**3**		1	97.3 (±0.5)	90.1 (±0.6)	93 (±1)
4	**4**		1	97.9 (±0.4)	86 (±1)	88 (±1)
5	**1**	H	2	95.7 (±0.7)	80.9 (±0.6)	84 (±1)
6	**2a**		2	95.9 (±0.1)	86 (±1)	90 (±1)
7	**3**		1	93.9 (±0.3)	90 (±2)	96 (±3)
8	**4**		1	94 (±2)	90 (±3)	96 (±5)
9	**1**	OMe	2	83.5 (±0.5)	54 (±2)	65 (±3)
10	**2a**		2	77.1 (±0.8)	69 (±3)	90 (±5)
11	**3**		3	76.7 (±0.2)	76.5 (±0.4)	99.7 (±0.8)
12	**4**		3	75.9 (±0.5)	74.4 (±0.3)	98 (±1)

[a] Reaction conditions: substrate (0.15 mmol), ^{i}PrOH (0.4 mL), catalyst (0.1 mol%) and KO^{t}Bu (0.625 mol%), 80 °C, and the reactions were monitored hourly until >90% of consumption of the substrate or no further reaction was observed. [b] Substrate consumptions and alcohol yields were determined by ^{1}H NMR spectroscopy in the presence of 1,3,5-trimethoxybenzene as an internal standard and performed in duplicate. The values reported are the average and the errors are reported in the parentheses. [c] (Yield/consumption) × 100. Absolute errors are provided in the parentheses.

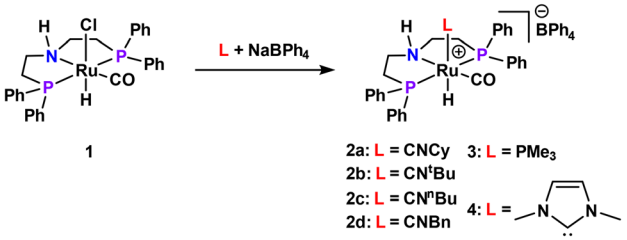

Scheme 1 Synthesis of **2a**, **2b**, **2c**, **2d**, **3** and **4**.

2a–d, **3**, and **4** were determined by NMR and FTIR spectroscopies, and SCXRD.

The solution NMR spectra of **2a–d**, **3**, and **4** share a few characteristic signals of the six coordinate Ru–H cations. The ^{1}H NMR spectra of all the complexes contains a signal for the hydride at −7.3 to −9.0 ppm ($^{2}J_{HP}$ = 15–19 Hz) which is significantly shifted to higher field with respect to neutral **1** (−15.1 ppm) and other neutral analogues containing halide or alkoxide *trans* ligands[9,26,27] supporting that the ligand exchange and cation formation have significant effect on the electronics of the metal center. The new complexes also exhibit singlets in their ^{31}P NMR spectra (57–59 ppm) supporting the complexes maintain C_s symmetry. The Ru–H signal in the ^{1}H NMR spectrum of **3** is a doublet of triplets with a large doublet coupling constant value of $^{2}J_{HP}$ = 86 Hz which is similar to other Ru–H with a *trans* PMe_3 ligand supports that the PMe_3 ligand is *trans* to the hydride and not *cis*.[25–27] Catalysts **2a–d**, **3**, and **4** were further studied by the FTIR spectroscopy to obtain electronic structure information.

The FTIR spectra of **2a–d** contain signals for the isonitrile (ν_{CN} = 2160–2178 cm^{-1}) ligands with stretching frequencies that are similar to the bis-isonitrile cations reported by Gauvin and coworkers (*cis* ν_{CN} = 2059 cm^{-1}, *trans* ν_{CN} = 2135 cm^{-1}),[24] supporting that these complexes are cations and the isonitrile ligands are *trans* to the hydride. The FTIR spectra of all 6 new complexes in this study contain a signal for the *trans* carbonyl (ν_{CO} = 1931–1961 cm^{-1}), which lie at frequencies similar to the *cis* CO of the bis-carbonyl cation reported by Prakash and coworkers (*cis* ν_{CO} = 1964 cm^{-1}, *trans* ν_{CO} = 2052 cm^{-1}).[28] In general, the complexes, **3** and **4**, containing strong σ-donating ligands exhibit lower FTIR ν_{CO} stretch frequencies due to the increased electron density as expected. The solid-state structures of **2b**, **2d**, **3** and **4** were further confirmed by SCXRD analyses (see ESI† for details).

The SCXRD structures (Fig. 2) indicate that the N–H is *anti* to the Ru–H in the solid state. The structure of the cation in the SCXRD structure of **3** is similar to the same previously published cation with alkoxide anions.[25] ^{1}H–^{1}H NOESY NMR experiments could not identify significant N–H and Ru–H correlations in any of the catalysts in this study supporting that the *anti*-isomer is the major species in solution as well. After analyzing the structures, we compared the catalytic activity of **2a–2d**, **3**, and **4** to **1** for ketone transfer hydrogenation reaction.

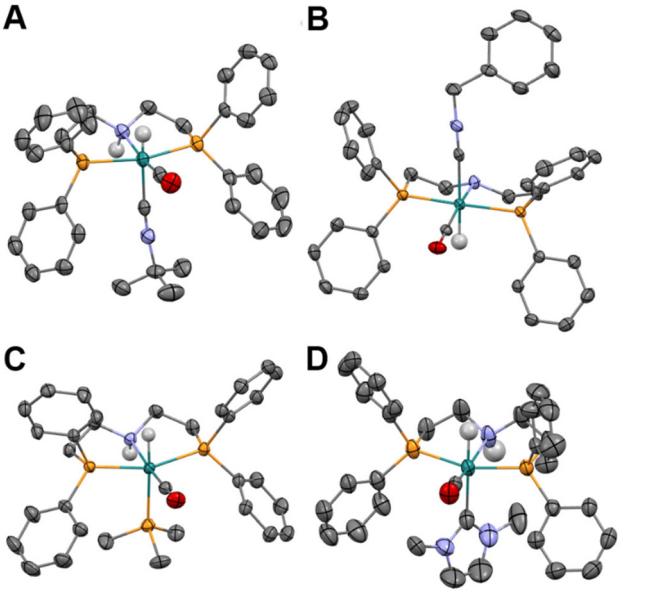

Fig. 2 SCXRD of **2b** (A), **2d** (B), **3** (C), and **4** (D), thermal ellipsoids are drawn at 50% probability. The BPh_4 anions, solvent molecules and most hydrogen atoms are omitted for clarity. See ESI† for further details.

Catalysis studies

1 and other Ru pincer complexes are well known to perform carbonyl reduction reactions, therefore we elected to benchmark the new complexes in this work in the transfer hydrogenation of ketones with isopropanol. To identify mechanistically viable reaction conditions, the reduction of benzophenone was performed with isopropanol and KO^{t}Bu as the base with **2a** as the catalyst (Table S1†). Catalyst loadings of 0.1 mol% of catalyst and 0.625 mol% of base in neat isopropanol were chosen to compare the different catalysts in this study with **1** (Table 1).

The alkyl isonitrile catalysts, **2a–2c**, exhibited comparable catalytic activities to **1**. The alkyl isonitriles were originally chosen to determine if the steric environment of the *trans* ligand effects the reactivity of the catalyst. However, no distinguishable trend was observed, indicating the structure of the ligand had little effect on the overall structure. On the other hand, **2d** is a much slower catalyst than **1**, showing that the electron withdrawing ligand reduces the catalysts activity for this reaction, supporting that the electronic environment of the ligand *trans* to the Ru–H has a strong effect on the catalytic activity. On the contrary, **3** and **4** are more active than **1** and **2a–2d**, supporting that σ-donating ligands enhance the catalyst activities. We hypothesize that the σ-donating ligands enhance the nucleophilicity of the Ru–H, speeding up the initial reaction with the substrate. To better understand the effects of the *trans* ancillary ligand on catalyst activity, selectivity, and stability we tested the transfer hydrogenation of functionalized acetophenones.

Functional group tolerance is a common challenge in catalysis; therefore, we examined the new catalysts abilities to

reduce acetophenones under similar conditions to compare their functional group tolerances to **1**. **1**, **2a**, **3**, and **4** were tested for the transfer hydrogenation of 4-bromoacetophenene, acetophenone, and 4-methoxyacetophenone with isopropanol (Table 2). For acetophenone, all four catalysts completed the reaction within 1–2 hours, with the electron rich **3** and **4** completing the reactions faster in general. Interestingly, **3** and **4** were notably more chemoselective than **1** (96 *vs.* 84%). The enhanced chemoselectivity differences are more pronounced for bromoacetophenone where **3** and **4** produce 4-bromo-α-methylbenzyl alcohol with selectivities of ~90%, whereas **1** and **2a** only generated the product with 62 and 72% selectivities, respectively. In the reduction of methoxyacetophenone, all 4 catalysts stopped consuming the ketone at ~75–84% conversion, suggesting the reactions reach an equilibrium. The selectivities for 4-methoxy-α-methylbenzyl alcohol were again low for **1** and high for **3** and **4** (65 *vs.* 99%). In general, the cation precursors were more chemoselective for the expected alcohol products. This may be attributed to the known instability of active intermediates of **1** in similar reactions.[25,29] The addition of a ligand *trans* to the Ru–H has been previously shown to improve the stability of **1**, forming neutral (PhPNP)Ru(H)(CO)(PR_3) and cationic $[(PhPN^HP)Ru(H)(CO)(PR_3)]^+$ complexes that are highly active alcohol dehydrogenation and ester hydrogenation catalysts.

Attempts to determine catalyst speciation

We hypothesized that the newly introduced ancillary ligands *trans* to the hydride remain bound to Ru during catalysis. However, the possibility remains that the improved activity and selectivities are the result of ligand stabilization of active species and requires the dissociation of the ligand to form the active species. The requirement of base in the catalysis also suggests that the active species may be a neutral species, such as (PhPNP)Ru(H)(CO) which was proposed by Schaub and coworkers by dissociation of PMe_3 from (PhPNP)Ru(H)(PMe_3)(CO).[25] Also, the active species in these types of reactions is generally believed to contain an NH *syn* to the hydride, which contributes to the complexes ability to perform metal–ligand cooperative reactions.[30] However, the complexes in this work contain *anti* motifs. Therefore, we performed a number of high catalyst loading and other reactions in an effort to determine the catalyst resting state and active speciation.

In isopropanol, **1** reacts with KO^{t}Bu (2.5 equiv.) to form multiple species based on NMR spectroscopy (see Fig. S13–S15†). $(PhPN^HP)Ru(H)_2(CO)$[18] forms in the initial reaction along with several unidentifiable species. After heating and addition of benzophenone the speciation changes at every step, consistent with previous reports. On the other hand, dissolution of **2b** or **3** in isopropanol followed by the addition of KO^{t}Bu (2.5 equiv.) results in only minor shifting of the ^{1}H and ^{31}P NMR chemical shifts (assigned **2b′** and **3′**, respectively, see Fig. S16–S21†). There is no indication of the formation of neutral (PhPNP)Ru(H)(L)(CO) species or other major species with significantly different structures, showing the stability of the cations. For example, the major species in the reactions with **3** contains ^{31}P NMR chemical shifts of 56.0 and −27.7 ppm, which are very similar to **3** (^{31}P NMR chemical shifts = 56.5 & −26.8 ppm in THF-d_8) and differ from (PhPNP)Ru(H)(PMe_3)(CO) (^{31}P NMR chemical shifts = 67.1 and −25.2 ppm in THF-d_8).[25] Also, the hydride signal in the ^{1}H NMR of **3′** has a chemical shift of −7.41 (*trans* $^2J_{PH}$ = 85.6 Hz) that is nearly identical to the hydride signal of **3** (−7.38 ppm, *trans* $^2J_{PH}$ = 85.6 Hz) and differs from (PhPNP)Ru(H)(PMe_3)(CO) (−8.02 ppm, $^2J_{PH}$ = 104.8 Hz).

This data suggests that the $[(PhPN^HP)Ru(H)(L)(CO)]^+$ ions are persistent in the presence of isopropanol. The small changes in chemical shift may be due to changing the solvent mixture or inversion of the NH from *anti* to *syn*, relative to the hydride (Scheme 2). Studies have shown that proton shuttling in pincer complexes is accelerated in alcoholic solvents, so it would not be surprising if inversion of the NH *via* deprotonation followed by re-protonation is facile in isopropanol.[31] The analogous $[(PhPN^HP)Ru(H)(PMe_3)(CO)][OR]$[25] complexes ([OR] = [OPh] and [OMe]) have similar NMR chemical shifts and coupling constants to **3** and **3′**, therefore anion exchange of the $[BPh_4]^-$ ion for an $[O^iPr]^-$ ion in **3′** cannot be ruled out. Also, transient neutral species may yet form as the active species and not be observable under catalytic conditions by NMR spectroscopy.

Schaub and coworkers observed hydrogenation and dehydrogenative coupling catalysis with the (PhPNP)Ru(H)(CO)(PR_3) complexes in the presence of excess PPh_3 (3–13 equivalents) with only slight reductions in catalysis rates with *in situ* combinations and isolated pre-catalysts. A summary of similar transfer hydrogenation catalysis attempts for transfer hydrogenation of benzophenone with **1**, **2a**, and **3** is provided in Table 3. In contrast to the hydrogenation and dehydrogenative coupling reactions, addition of PMe_3 (1.4 equiv.) to **1** under the same transfer hydrogenation conditions in Table 1, entry 1 resulted in a significant reduction in catalysis (Table 3, entry 1). Similarly, *in situ* combinations of **1**, PMe_3 (1 equiv.), and $NaBPh_4$ (1 equiv.) resulted in no observed catalysis. These observations may be due to comparatively slow reactions of PMe_3, and $NaBPh_4$ with **1** under catalytic conditions due to low concentrations and competitive side reactions, such as $[(PhPN^HP)Ru(H)(CO)]_2[BPh_4]_2$ dimer formation or other unknown reactions. Addition of 1 or 5 equivalents of PMe_3 to **3** under catalytic conditions resulted in mere 25% and 0% yields of diphenylmethanol, respectively. The same loss in activity was observed with **2a** in the presence of excess CyNC. NMR spectroscopy of Table 3, entry 5 shows no change in the catalyst speciation in the presence of excess PMe_3 (Fig. S10–S12†).

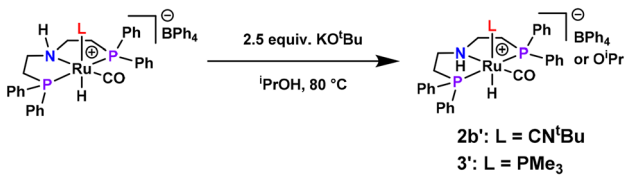

Scheme 2 Proposed reactions of **2b** and **3** with KO^{t}Bu in ^{i}PrOH.

This suggests that the ligand may need to dissociate to form the active catalysts and transfer hydrogenation is more sensitive to the presence of excess ligand than hydrogenation and dehydrogenative coupling catalyses.

To confirm the ligands *trans* to the hydride are labile, we attempted to exchange the ligands in **2b** and **4** with PMe_3 (1.1 equiv.). No exchange was observed in the presence of isopropanol (30 equiv.) (Fig. S83–S88†). However, upon introduction of base, some exchange and **3′** was observed with heating at 80 °C. This suggests that the ligands *trans* to the hydride may dissociate when exposed to catalytic conditions, however more studies will be required to determine if this observation is relevant to the transfer hydrogenation of ketones and other catalytic reactions.

At high catalyst loadings (2 mol% Ru) of **2b** or **3** the NMR signals of the catalysts are similar to the starting complexes in THF-d_8 indicating minimal changes to the chemical structures of the $[(PhPN^HP)Ru(H)(CO)(L)]^+$ ions. The observed species are likely off-cycle, catalyst resting states. The addition of extra ligand during catalysis suggests that the mechanism may require dissociation of the ligand *trans* to the hydride to form the active species and the improved chemoselectivities of these complexes is due to stabilization of the active speces by the labile ligand. However, the significant activity increases of **3** and **4** over **1** suggest the mechanism may be more complicated or the active species is the $[(PhPN^HP)Ru(H)(CO)]^+$ ion under these conditions. More studies, including computations, will be necessary to definitively determine the speciation of $[(PhPN^HP)Ru(H)(CO)(L)][BPh_4]$ in transfer hydrogenation catalysis conditions.

Conclusions

In this work, a series of cationic Ru pincer complexes were synthesized *via* ligand substitution of the chloride in Ru–MACHO followed by anion exchange to study the effects of the ancillary ligand *trans* to the Ru–H bond. NMR spectroscopy and SCXRD revealed that all 6 new catalysts contained an N–H that was *anti* to the Ru–H and the new ancillary ligand was *trans* to the Ru–H allowing for direct comparisons. The complexes catalyze the transfer hydrogenation of ketones utilizing isopropanol as the hydrogen source. In general, electron poor, π-accepting ligands resulted in slower catalysis, whereas sigma donors accelerated the catalysis compared to Ru–Macho. The additional ligands improved the chemoselectivity of the transfer hydrogenation of acetophenones, especially for functionalized acetophenones. These studies contribute to the continuing understanding of pincer complex reactivity and design principles for building more active and stable catalysts.

Author contributions

All authors contributed to the project design. M.H., D.C.C., and A.M.C. performed the laboratory syntheses, catalysis, and spectroscopic characterizations. The manuscript was written through contributions by all authors. All authors have given approval to the final version of the manuscript.

Data availability

Crystallographic data for the structures reported in this article have been deposited at the Cambridge Crystallographic Data Centre under deposition numbers 2392950–2392953.† NMR spectra and other data are provided in the ESI† associated with this publication.

Conflicts of interest

There are no conflicts to declare.

Acknowledgements

This research was supported by the U.S. Department of Energy, Office of Science, Office of Basic Energy Sciences, Chemical Sciences, Geosciences, and Biosciences Division, Catalysis Science program. Ames National Laboratory is operated for the U.S. Department of Energy by Iowa State University under Contract No. DEAC02-07CH11358. D. C. C.'s contribution was supported by the U.S. Department of Energy, Office of Science, Office of Workforce Development for Teachers and Scientists (WDTS) under the Science Undergraduate Laboratory Internships Program (SULI). Part of A.M.C.'s contribution was supported by Ames National Laboratory under the Strategic Partnership Program 2024-01 with Iowa State University. Part of the purchase of the AVIII-600 NMR spectrometer used to obtain results included in this publication was supported by the National Science Foundation under Grant No. MRI 1040098. Purchase of the 400 MR NMR spectrometer used to obtain results included in this publication was supported by the National Science Foundation under Grant No. CHE 0946687. Any opinions, findings, and conclusions or recommendations expressed in this material are those of the author(s) and do not necessarily reflect the views of the National Science Foundation. The Single Crystal X-Ray structure determinations were performed in the Molecular Structure Lab of the Chemistry Department of Iowa State University by Dr Arkady Ellern.

References

1 C. Gunanathan and D. Milstein, *Chem. Rev.*, 2014, **114**, 12024–12087.
2 H. A. Younus, W. Su, N. Ahmad, S. Chen and F. Verpoort, *Adv. Synth. Catal.*, 2015, **357**, 283–330.
3 L. Piccirilli, D. Lobo Justo Pinheiro and M. Nielsen, *Catalysts*, 2020, **10**, 773.

4 D. A. Ekanayake and H. Guan, in *Met.-Ligand Co-Oper. Catal. Pincer-Met. Platf*, ed. G. van Koten, K. Kirchner and M.-E. Moret, Springer International Publishing, Cham, 2021, pp. 263–320.
5 B. G. Reed-Berendt, D. E. Latham, M. B. Dambatta and L. C. Morrill, *ACS Cent. Sci.*, 2021, **7**, 570–585.
6 J. Hafeez, M. Bilal, N. Rasool, U. Hafeez, S. Adnan Ali Shah, S. Imran and Z. Amiruddin Zakaria, *Arabian J. Chem.*, 2022, **15**, 104165.
7 K. K. Manar, J. Cheng, Y. Yang, X. Yang and P. Ren, *ChemCatChem*, 2023, e202300004.
8 W. Kuriyama, T. Matsumoto, O. Ogata, Y. Ino, K. Aoki, S. Tanaka, K. Ishida, T. Kobayashi, N. Sayo and T. Saito, *Org. Process Res. Dev.*, 2012, **16**, 166–171.
9 M. Bertoli, A. Choualeb, A. J. Lough, B. Moore, D. Spasyuk and D. G. Gusev, *Organometallics*, 2011, **30**, 3479–3482.
10 S. Schneider, J. Meiners and B. Askevold, *Eur. J. Inorg. Chem.*, 2012, **2012**, 412–429.
11 R. A. Farrar-Tobar, Z. Wei, H. Jiao, S. Hinze and J. G. de Vries, *Chem. – Eur. J.*, 2018, **24**, 2725–2734.
12 T.-O. Kindler, C. Alberti, E. Fedorenko, N. Santangelo and S. Enthaler, *ChemistryOpen*, 2020, **9**, 401–404.
13 Y. Shaalan, L. Boulton and C. Jamieson, *Org. Process Res. Dev.*, 2020, **24**, 2745–2751.
14 F. L. Kirlin, O. J. Borden, M. C. Head, S. E. Kelly and A. R. Chianese, *Organometallics*, 2022, **41**, 1025–1033.
15 D. B. Culver and J. M. Boncella, *ChemCatChem*, 2023, **15**, e202201587.
16 B. Askevold, M. M. Khusniyarov, W. Kroener, K. Gieb, P. Müller, E. Herdtweck, F. W. Heinemann, M. Diefenbach, M. C. Holthausen, V. Vieru, L. F. Chibotaru and S. Schneider, *Chem. – Eur. J.*, 2015, **21**, 579–589.
17 O. Ogata, Y. Nakayama, H. Nara, M. Fujiwhara and Y. Kayaki, *Org. Lett.*, 2016, **18**, 3894–3897.
18 L. Zhang, G. Raffa, D. H. Nguyen, Y. Swesi, L. Corbel-Demailly, F. Capet, X. Trivelli, S. Desset, S. Paul, J.-F. Paul, P. Fongarland, F. Dumeignil and R. M. Gauvin, *J. Catal.*, 2016, **340**, 331–343.
19 D. B. Culver and J. M. Boncella, *Inorg. Chem.*, 2023, **62**, 19383–19388.
20 S. Luo, H. D. M. Pham, C.-C. Li, Z. Qiu, R. Cheng, R. Z. Khaliullin and C.-J. Li, *Org. Lett.*, 2024, **26**, 3004–3009.
21 S. S. Rozenel and J. Arnold, *Inorg. Chem.*, 2012, **51**, 9730–9739.
22 S. Kar, R. Sen, J. Kothandaraman, A. Goeppert, R. Chowdhury, S. B. Munoz, R. Haiges and G. K. S. Prakash, *J. Am. Chem. Soc.*, 2019, **141**, 3160–3170.
23 O. Ogata, Cationic Ruthenium Complex, and Production Method Therefor and Use Thereof, WO2018181865, 2018.
24 D. H. Nguyen, D. Merel, N. Merle, X. Trivelli, F. Capet and R. M. Gauvin, *Dalton Trans.*, 2021, **50**, 10067–10081.
25 D. J. Tindall, M. Menche, M. Schelwies, R. A. Paciello, A. Schäfer, P. Comba, F. Rominger, A. S. K. Hashmi and T. Schaub, *Inorg. Chem.*, 2020, **59**, 5099–5115.
26 A. Friedrich, M. Drees, M. Käss, E. Herdtweck and S. Schneider, *Inorg. Chem.*, 2010, **49**, 5482–5494.
27 M. Käß, A. Friedrich, M. Drees and S. Schneider, *Angew. Chem., Int. Ed.*, 2009, **48**, 905–907.
28 S. Kar, R. Sen, J. Kothandaraman, A. Goeppert, R. Chowdhury, S. B. Munoz, R. Haiges and G. K. S. Prakash, *J. Am. Chem. Soc.*, 2019, **141**, 3160–3170.
29 V. Krishnakumar, B. Chatterjee and C. Gunanathan, *Inorg. Chem.*, 2017, **56**, 7278–7284.
30 J. R. Khusnutdinova and D. Milstein, *Angew. Chem., Int. Ed.*, 2015, **54**, 12236–12273.
31 N. E. Smith, W. H. Bernskoetter and N. Hazari, *J. Am. Chem. Soc.*, 2019, **141**, 17350–17360.